MICROPHONICS SUPPRESSION STUDY IN ARIEL e-LINAC CRYOMODULES*

Yanyun Ma[†], K. Fong, J. Keir, D. Kishi, S.R. Koscielniak, D. Lang, S. Liu,
R.E. Laxdal, R.S. Sekhon, X. Wang
TRIUMF, Vancouver, BC, Canada

Abstract

Now the stage of the 30 MeV portion of ARIEL (The Advanced Rare Isotope Laboratory) e-Linac (1.3 GHz, SRF) is under commissioning which includes an injector cryomodule (ICM) with a single nine-cell cavity and the 1st accelerator cryomodule (ACM1) with two cavities configuration. The two ACM1 cavities are driven by a single klystron with vector-sum control and running in CW mode. We have observed a ponderomotive instability in ACM1 driven by the Lorentz force and seeded through microphonics that impacts beam stability [1-5]. Extensive damping has been implemented during a recent shutdown. The beam test results show 20 MeV acceleration gain can be reached by ACM1. A fast piezoelectric (Piezo) tuner is under development to allow a fast tuning compensation for the e-Linac cavities. In this paper, the progress of the microphonics suppression of Cryomodules is presented.

INTRODUCTION

ARIEL e-Linac is a continuous-wave (CW) superconducting electron linear accelerator. The accelerator is divided into three cryomodules [6, 7]: an ICM with one cavity and two ACM with two 1.3 GHz nine-cell cavities each. The 'Demonstrator' phase of ARIEL was installed for initial technical and beam tests with successful beam acceleration to 22 MeV [8]. The ACM1 cryomodule, initially installed with one cavity, was then updated to 2 cavities [9] but still driven by a single klystron in vector sum. During commissioning, acoustic noise from the environment vibration generated by the cooling water system, cooling air, cryogenic system and vacuum system seeded a coupled cavity instability driven by the Lorentz force that impacted the ACM1 rf performance and final beam energy stability. The final energy gain of ACM1 was limited to around 17~18 MeV with significant energy instability [1]. Extensive damping has been implemented during a recent shutdown. The new test results show 30 MeV beam has been achieved after ACM1 which energy gain is about 20.6 MeV.

PONDERMOTIVE EFFECT

Both ICM and ACM1 work in phase-locked loop (PLL) self-excited loop (SEL) in CW mode. Unlike the ICM with one cavity and one SEL loop, the two ACM1 cavities are driven by a single klystron with vector-sum control of the two cavity SEL PLL. There is no gradient regulation for each individual cavity in the ACM1 [10]. Individual tuner

loops are established to maintain the cavity frequency with respect to the established reference phases. Microphonics can excite mechanical resonances in either cavity, perturbing the RF resonant frequency, which can couple to the other cavity via vector-sum regulation. The resonance modulations lead to further amplitude variations in the two cavities which in turn drive the mechanical resonances, leading to a ponderomotive instability [11-15].

While under vector-sum regulation, the ACM1 cavities pickup signals indicated a slowly developing (over seconds), large amplitude oscillation at about 160 Hz in counterphase (Fig. 1) impacting the energy stability and ultimately the loop stability.
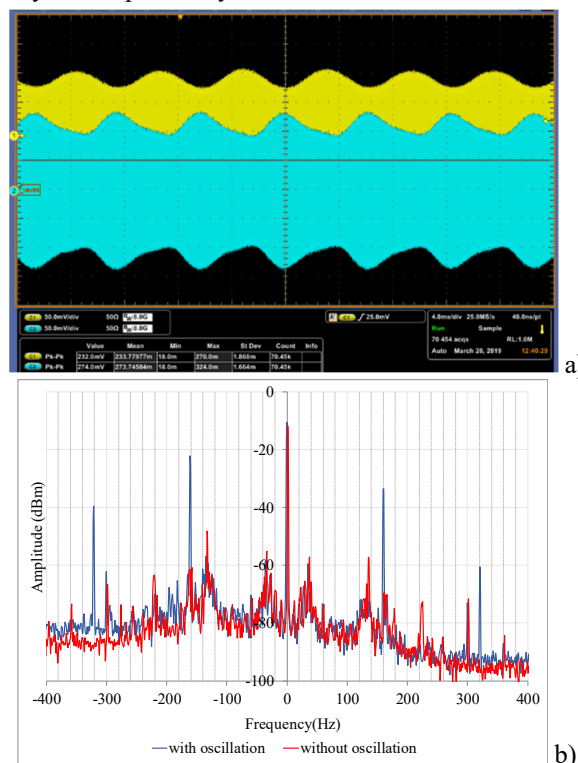

a)

b)

Figure 1: The two-cavity oscillation of ACM1 pickup signals. (a) The yellow & cyan waveforms are the 1st and 2nd cavity pickup signals, respectively. (b) Without oscillation, the 160 Hz peak is not notable(red). When the oscillation happens, the 160 Hz peak becomes much stronger(blue).

The field threshold for excitation of this instability is impacted both by ambient microphonic noise that can seed the instability and the precise settings of the two cavity phase loops. The coupled oscillation can deteriorate the e-Linac final energy stability outside specification and needs to be controlled.

MICROPHONICS SOURCE SEARCHING AND DAMPING

The external vibrations couple to the mechanical system constituted by the cavity and auxiliary components and excite mechanical modes at resonance.

RF Waveguide System Damping

The e-Linac high power RF system consists of two klystrons, six high power dummy loads, two circulators and waveguide components. The water system cooling these components comprises the main vibration source for the RF system. The vibration source of the water-cooling system and their solutions are as follows.

1) Each klystron collector requires approximately 500 L/min of cooling water, provided by individual booster pumps. The two booster pumps generate large vibrations during operation, reside in the accelerator hall and have no vibration damping. The design of damping for the pumps is under development.

2) The waveguide support and the klystrons were upgraded from floating supports to anchored supports with the ground.

3) The turbulent water flows for klystrons and dummy load also generate vibrations in the water-cooled RF devices. All waveguide components and dummy loads are damped with respect to the waveguide supports. Four of the dummy loads are clamped to the ground or shielding blocks through individual supports. To damp the vibration near the source, the waveguides directly attached to the dummy loads are clamped to the waveguide supports with 50 Duro Sorbothane®. To reduce the vibration transmission through the waveguide to the cryomodule, the waveguides are clamped to the shielding blocks at both the horizontal section and vertical section with 50 Duro Sorbothane® as illustrated in Fig. 2.

4) All the rubber hoses between stainless steel water pipes and RF devices were installed snug due to aesthetic reasons. Mechanical vibrations from the water system were transmitted to waveguides through tight hoses. All the tight hoses were replaced with longer hoses to reduce the transmission as illustrated in Fig. 3 for ACM1 circulator load, circulator and power divider load.

5) During the initial installation some of the rubber hoses and stainless-steel water pipes were mechanically connected to the waveguide supports. These are now separated from the waveguide supports. Figure 4 shows the improvements after the stainless-steel water pipes are disconnected from the coupler support stand.

Accelerometers (Dytran 3100D24T) and dynamic signal analyzer (Agilent 35670A) are used to compare damping effects during implementation.
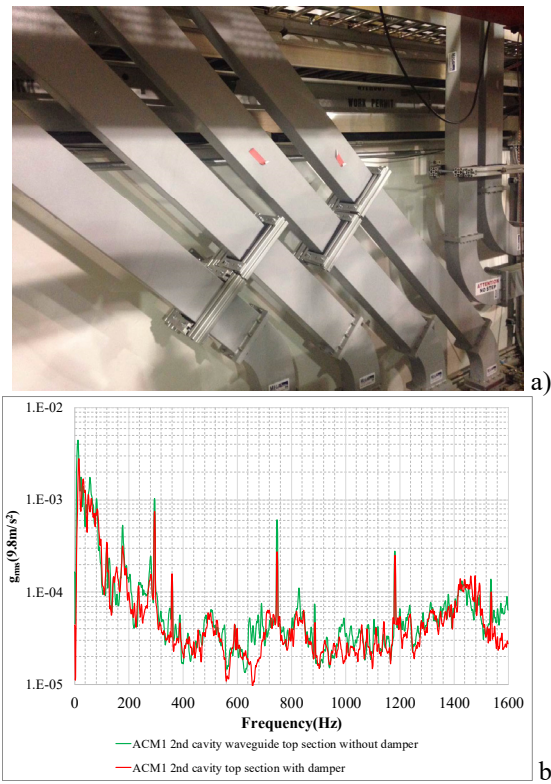

Figure 2: ACM1 waveguide damping (a) ACM1 waveguides clamped to the shielding blocks with separate clamps made of Bosch profiles with Sorbothane® inserted between the clamp and waveguide. (b) Accelerometer results from the 2nd cavity waveguide top section without (green) and with (red) clamped damper. After damping almost all the vibration peaks become lower.
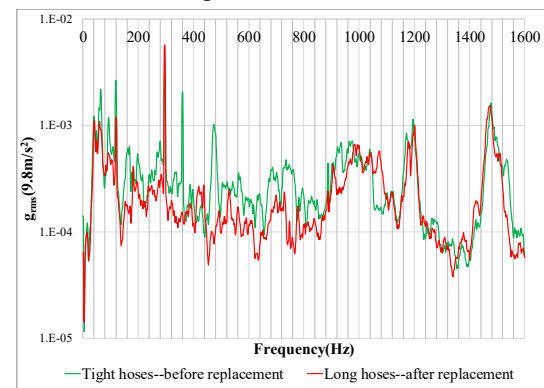

Figure 3: Accelerometer data before (green) and after (red) ACM1 circulator load, circulator and power divider load hoses replacement. Both curves were obtained under same conditions with water pumps running. Almost all peaks are reduced after the tight hose replacement except the 297 Hz which corresponds to the water pumps and keeps almost no change.
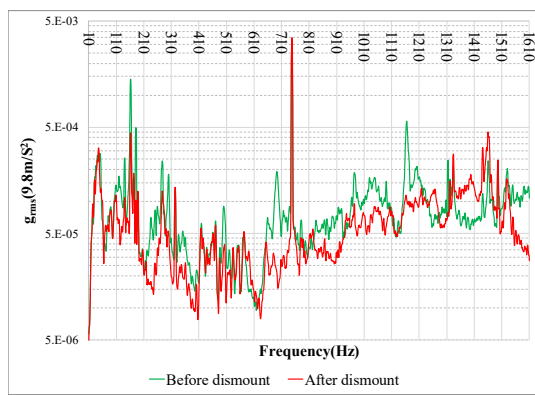
Figure 4: Before (green) and after (red) disconnecting ACM1 1st east coupler water-cooling SS pipes from the support stand. Both curves were obtained under the same conditions with Turbo pumps running. Most of the vibration peaks are reduced except 750 Hz which corresponds with Turbo pumps and keeps almost no change.

RF Couplers Cooling Air

A total of 4 RF couplers (CPI VWP 3032) for two cavities are installed in ACM1. The warm windows are cooled by about 100 L/m compressed air. Vibration measurements show that the air flow increases noise above 180 Hz [2]. To optimize the cooling-air flow rate and monitor the temperature of the warm window a temperature sensor (OS36-T-140F) has been installed in each coupler. After the air flow reduction, the couplers warm window temperatures increase by ~10 K with 5 kW standing wave mode.

Vacuum System

Two turbo pumps are installed on the cryomodule lid to establish the isolation vacuum. The turbo pumps and the roughing pump have been identified as vibration sources [1~2]. After 2K cooldown, the phase noise of ACM1 pickup signal has been measured with one turbo pump off as shown in Fig.5. Based on the test results, both Turbo pumps and the roughing pump have been turned off once the cavities are at 2K.
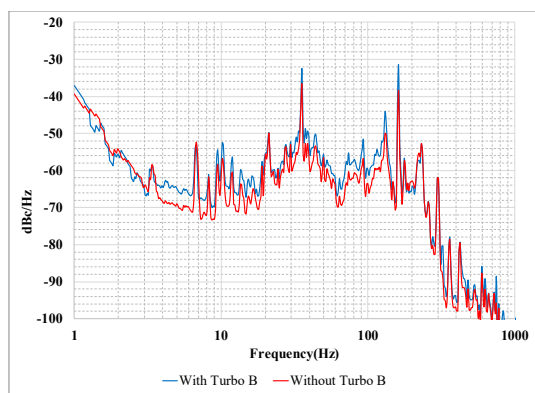

Figure 5: ACM1 1st cavity pickup signal phase noise with (blue) and without (red) turbo pump 'B' under 20 MV vector sum mode measured by Keysight E5052B. With one Turbo pump off, almost all the peaks are lower.

LN System Upgrade

The cold mass and coupers are thermally isolated using LN2-cooled shell and piping. During initial commissioning the beam energy disturbances were correlated with the LN2 valve status [1]. The LN2 phase separator was filled by a solenoid valve that opens when the level reaches 30% and closes at 80%. The cryomodule LN2 supply valve was controlled by the GN2 exhaust temperature with a long latency time.

A flow proportional valve has been added for the LN2 phase separator level regulation and the cryomodule LN2 supply valve is now regulated from the RF coupler LN2 intercept temperature with a sensor close to the RF coupler cold window. The LN2 system is now more stable with further improvements expected through optimization of the PID control loops.

PIEZO TUNER TEST

A piezoelectric (Piezo) tuner which allows a fast compensation for mechanical detuning is currently under development. The Piezo unit is inserted into the scissor tuner warm assembly of the ICM. The Piezo actuator with part number P-830.20 (30 µm travel range, 1000 N / 5 N) and amplifier with part number E617.001 are employed [16,17]. The transfer function of the ICM is shown in Fig. 6.
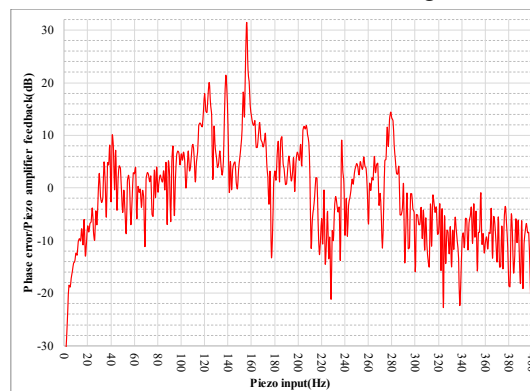

Figure 6: Transfer function of ICM which is obtained by sweeping the Piezo drive from 0Hz up to 400 Hz with 3 MV/m gradient while measuring the phase loop error by Agilent 35670 A. The 156 Hz has strongest detuning.

A shaker has been set up on ICM lid as an external vibration source. The feedback of phase loop error signal is used as Piezo drive signal with 180 degrees phase shift. During the test the shaker was driven by an individual signal generator at 156 Hz. Preliminary test results show the strongest detuning peak which is 156 Hz can be suppressed by the Piezo tuner by a factor of 7 in phase error and 10 dB in amplitude spectrum as shown in Fig. 7.
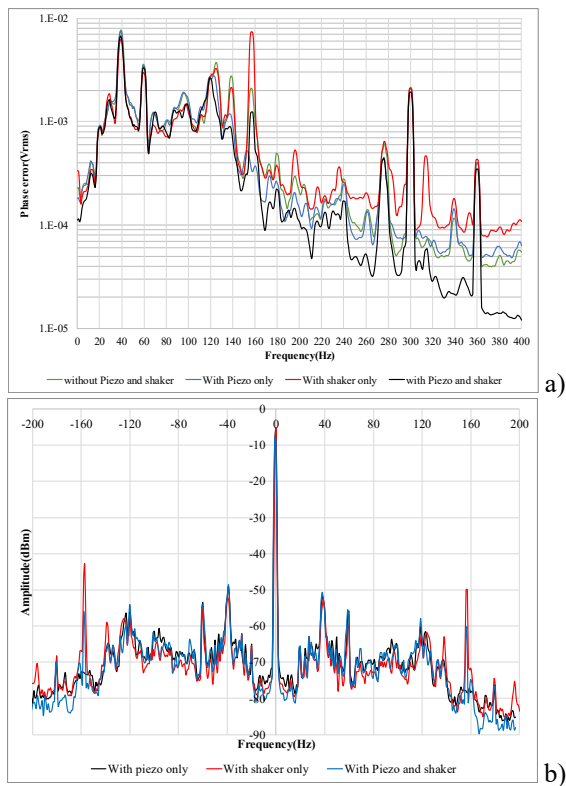
a)

b)

Figure 7: Effect of active microphonics compensation on ICM. (a) The phase error of ICM without Piezo and shaker (green), with Piezo only (blue), with shaker only (red) and with Piezo and shaker (black). (b) The spectrum of ICM pick up signal with Piezo only (black), with shaker only (red) and with Piezo and shaker (blue).

RF AND BEAM TEST RESULTS

The single cavity mode phase noise test results before and after damping show that the microphonics have been reduced as shown in Fig. 8. The low frequency noise floor (<10Hz) increases and the effect of it is under study. 20 MV has been achieved in ACM1 under vector sum mode as shown in Fig. 9.
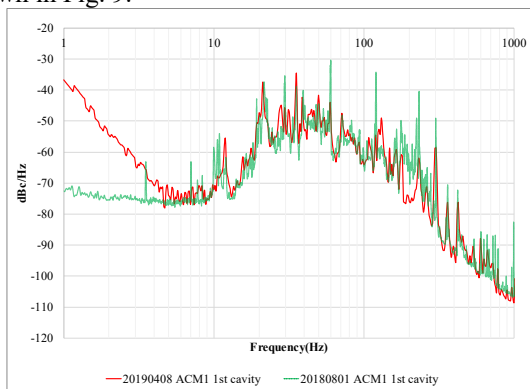

Figure 8: ACM1 1st cavity pickup signal phase noise before (green) and after (red) damping campaign at 8.5 MV/m single cavity mode. Most peaks have been reduced.

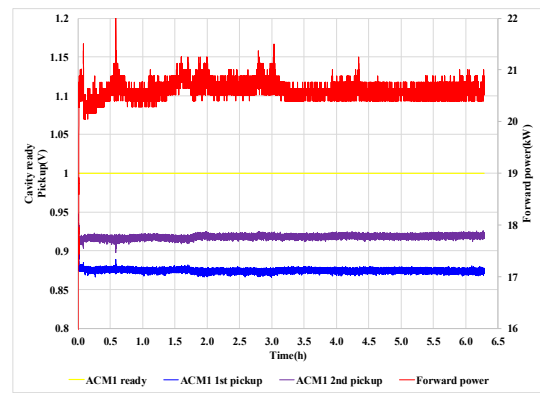Figure 9: ACM1 at 20 MV vector sum mode. Forward power in red, 'ready' signal (amplitude, phase and tuner loops are locked) in yellow, 1st cavity pickup signal in blue and 2nd cavity pickup in purple.
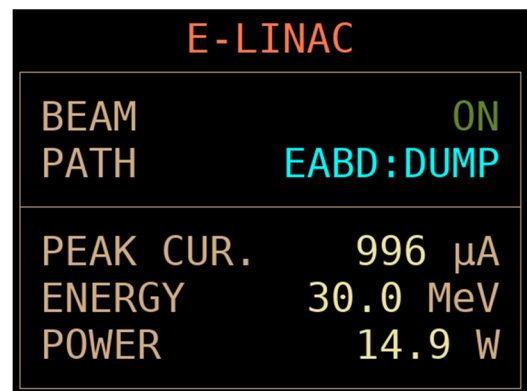

Figure 10: ACM1 output beam parameters.

The beam has been delivered through ICM and ACM1 with output energy 9.4 MeV and 30 MeV respectively as shown in Fig.10. The voltage gain of ACM1 is about 20.6 MV.

ACKNOWLEDGEMENTS

REFERENCES

[1] Y. Ma *et al.*, "Microphonics Investigation of ARIEL e-Linac Cryomodules", in Proc. 29th Linear Accelerator Conf. (LINAC'18), Beijing, China, Sep. 2018, pp. 370-373. doi:10.18429/JACoW-LINAC2018-TUPO020

[2] Y. Ma, "Microphonics Study of ARIEL ACM1 Two Cavities Cryomodule", MRCW18, Brooklyn, NY, USA.
https://indico.bnl.gov/event/4460/contributions/24516/attach-ments/20461/27438/MICROPHON-ICS_STUDY_OF_ARIEL_ACM1_TWO_CAVI-TIES_CRYOMODULE.pdf

[3] Y. Ma, "Microphonics measurements on ARIEL E-linac Cryomodule", TTC2019, Vancouver, Canada. Feb. 2019. https://indico.desy.de/indico/event/21337/session/20/contribution/99

[4] S. R. Koscielniak *et al.*, "Status and Issues (Microphonics, LFD, MPS) with TRIUMF ARIEL e-Linac Commissioning", in *Proc. 29th Linear Accelerator Conf. (LINAC'18)*, Beijing, China, Sep. 2018, pp. 286-291. `doi:10.18429/JACoW-LINAC2018-TU1A03`

[5] Y. Ma *et al.*, "Microphonics Suppression in ARIEL ACM1 Cryomodule", in *Proc. 10th Int. Particle Accelerator Conf. (IPAC'19)*, Melbourne, Australia, May 2019, paper MOPGW004, pp. 65-68, `https://doi.org/10.18429/JACoW-IPAC2019-MOPGW004`

[6] S. R. Koscielniak *et al.*, "Electron Linac Photo-fission Driver for the Rare Isotope Program at TRIUMF", in *Proc. 1st Int. Particle Accelerator Conf. (IPAC'10)*, Kyoto, Japan, May 2010, paper THPD001, pp. 4275-4277.

[7] R.E. Laxdal *et al,* "The Injector Cryomodule for e-Linac at TRIUMF", AIP Conf. Proc. 1434, 969 (2012); http://dx.doi.org/10.1063/1.4707014

[8] M. Marchetto *et al.*, "Commissioning and Operation of the ARIEL Electron Linac at TRIUMF", in *Proc. 6th Int. Particle Accelerator Conf. (IPAC'15)*, Richmond, VA, USA, May 2015, pp. 2444-2449. `doi:10.18429/JACoW-IPAC2015-WEYC3`

[9] Y. Ma *et al.,* "First RF Test Results of Two-Cavities Accelerating Cryomodule for ARIEL eLinac at TRIUMF", in *Proc. 9th Int. Particle Accelerator Conf. (IPAC'18),* Vancouver, Canada, Apr.-May 2018, pp. 4512-4515. doi:10.18429/JACoW-IPAC2018-THPMK090

[10] K. Fong, Z. T. Ang, M. P. Laverty, and Q. Zheng, "Tuners Alignment on Two 9-Cell Cavities with Single Amplifier under Self-Excited Loop", in *Proc. 9th Int. Particle Accelerator Conf. (IPAC'18)*, Vancouver, Canada, Apr.-May 2018, pp. 4527-4529. doi:10.18429/JACoW-IPAC2018-THPMK096

[11] R. Leewe, "LLRF compensation and mitigation of two cavity instability". TTC2019, Vancouver, Canada. Feb. 2019, https://indico.desy.de/indico/event/21337/session/6/contribution/33/material/slides/0.pdf

[12] R. Leewe, "Coupled Mechanical Oscillations in Multiple Cryomodule Driven by a Single Klystron". MRCW18, Brooklyn, NY, USA.
https://indico.bnl.gov/event/4460/contributions/24545/attachments/20454/27370/Microphonics2018.pdf

[13] K. Fong and R. Leewe, "Parametric Pumped Oscillation by Lorentz Force in Superconducting Rf Cavity", in *Proc. 10th Int. Particle Accelerator Conf. (IPAC'19)*, Melbourne, Australia, May 2019, paper WEPRB003, pp. 2798-2800, `doi:10.18429/JACoW--WEPRB003`

[14] S. R. Koscielniak, "Ponderomotive Instability of Two Self-Excited Cavities", in *Proc. 10th Int. Particle Accelerator Conf. (IPAC'19)*, Melbourne, Australia, May 2019, paper THPRB008, pp. 3812-3815, `doi:10.18429/JACoW--THPRB008`

[15] S. R. Koscielniak, "Vector Sum & Diffference Control of SRF Cavities", in *Proc. 10th Int. Particle Accelerator Conf. (IPAC'19)*, Melbourne, Australia, May 2019, paper THPRB009, pp. 3816-3819, `doi:10.18429/JACoW--THPRB009`

[16] https://www.pionline.it/fileadmin/user_upload/physik_instrumente/files/datasheets/E617-Datasheet.pdf

[17] https://static.physikinstrumente.com/fileadmin/user_upload/physik_instrumente/files/datasheets/P-810-P-830-Datasheet.pdf?_ga=2.37446560.1227748908.1555267108-191402797.1555267108